The wetting of planar solid surfaces by symmetric binary mixtures near bulk gas–liquid coexistence

2004 J. Phys.: Condens. Matter 16 4761

(http://iopscience.iop.org/0953-8984/16/28/002)

INSTITUTE OF PHYSICS PUBLISHING JOURNAL OF PHYSICS: CONDENSED MATTER

J. Phys.: Condens. Matter **16** (2004) 4761–4783 PII: S0953-8984(04)79734-9

The wetting of planar solid surfaces by symmetric binary mixtures near bulk gas–liquid coexistence

Dirk Woywod and Martin Schoen[1]

Stranski–Laboratorium für Physikalische und Theoretische Chemie, Sekretariat TC 7, Technische Universität Berlin, Straße des 17. Juni 124, D-10623 Berlin, Germany

E-mail: dirk.woywod@fluids.tu-berlin.de and martin.schoen@fluids.tu-berlin.de

Received 22 April 2004
Published 2 July 2004
Online at stacks.iop.org/JPhysCM/16/4761
doi:10.1088/0953-8984/16/28/002

Abstract

We investigate the wetting of planar, nonselective solid substrates by symmetric binary mixtures where the attraction strength between like molecules of components A and B is the same, that is $\epsilon_{AA} = \epsilon_{BB} < 0$. Mixture properties come about by varying $|\epsilon_{AB}| \leqslant |\epsilon_{AA}|$, that is by varying the attraction between a pair of unlike molecules. By means of mean-field lattice density functional calculations we observe a rich wetting behaviour as a result of the interplay between ϵ_{AB} and the attraction of fluid molecules by the solid substrate ϵ_W. In accord with previous studies we observe complete wetting only above the critical end point if the bulk mixture exhibits a moderate to weak tendency to liquid–liquid phase separation even for relatively strong fluid–substrate attraction. However, in this case layering transitions may arise below the temperature of the critical end point. For strongly phase separating mixtures complete wetting is observed for *all* temperatures $T \geqslant 0$ along the line of discontinuous phase transitions in the bulk.

1. Introduction

The study of wetting phenomena has a long history going back all the way to the works by Young [1] and later on by Dupré [2], who analysed the interaction of fluid with solid surfaces from a macroscopic perspective. In their analyses the contact angle θ of a sessile droplet on a solid surface was linked to various interfacial tensions such that if $\theta = 0$ one has *complete* wetting, that is a macroscopic film of liquid spreading over the entire substrate. If, on the other hand, one is dealing with stable droplets, $0 < \theta < \pi$, which is the case usually referred to as *partial* wetting. Since then a lot of experimental and theoretical work has been devoted to studying the wetting of solid surfaces by fluid matter [3–8]. Wetting is ubiquitous and important in a variety of contexts. For example, the way in which fluid molecules interact with

[1] Author to whom any correspondence should be addressed.

solids ultimately determines how paints stick to surfaces or how stains can be removed from fabric by detergents [9].

One of the first attempts to classify systems with respect to their wetting behaviour is the study by Dash, who analysed experimental sorption isotherms of physisorbed gases [10]. However, it was not until the seminal papers by Cahn [11] and Ebner and Saam [12, 13] that wetting phenomena were perceived as a novel class of phase transitions driven by the symmetry-breaking presence of a solid surface. Cahn has given a lucid argument in which he expresses $\cos\theta \propto t^{\beta-2\nu}$, where $t = (T_c - T)/T_c$ (T_c bulk gas–liquid critical temperature); β and ν are critical exponents associated with the density difference between coexisting liquids and gases and the range of intermolecular correlations, respectively [11]. Since $\beta - 2\nu < 0$ for two- and three-dimensional systems [14] a wetting temperature $T_w < T_c$ must exist where $\theta = 0$ such that we have complete wetting for all $T \geqslant T_w$.

While Cahn's argument is correct for short-range fluid–substrate potentials [6], it may be wrong for long-range potentials, as pointed out by Nightingale and Indekeu [15] and corroborated later by Ebner and Saam [16]. The importance of the range of fluid–substrate interactions and its relation to the order of the wetting transition was studied systematically in a number of papers [17–20]. For example, long-range fluid–substrate interactions are crucial for prewetting, that is coexistence between films of different but microscopic thicknesses since they lower the so-called roughening temperature below T_w (see also section 5.1) [21].

Since then it was realized that even the formation of individual layers of physisorbed molecules may constitute a discontinuous (i.e., *first-order*) phase transition. These so-called layering transitions were investigated by Pandit *et al* [22] who built on the earlier work by Dash [10]. The relation between wetting and layering transitions was investigated by Binder and Landau [23], who employed Monte Carlo simulations of Ising magnets on a simple-cubic lattice. These latter authors also give an account of the limitations of models with short-range interactions. In particular, they show that layering transitions and wetting, which are of prime interest in this study, are captured in a qualitatively correct way by such models.

While most of the work on wetting still deals with pure fluids, a considerable body of literature has addressed the issue of binary mixtures and their interaction with solid substrates. Of these papers, the larger portion focuses on mixtures *confined* by solid substrates to spaces of nanoscopic dimension(s) where wetting is subdominant to confinement-controlled phase transitions [24–27]. Wetting of solid surfaces by binary mixtures has, however, been studied by Patrykiejew *et al* [28] by means of lattice Monte Carlo simulations of associating binary mixtures. Again, these authors employ a long-range fluid–substrate potential. Monte Carlo simulations have also been employed by Kierlik *et al*, who concentrate on prewetting of a selective solid surface by a symmetric binary mixture where like particles of either component are solely distinguished by their 'colour' [29], that is the attraction between a pair of like molecules of both components is equally strong.

Experimentally, prewetting by the binary mixture methanol–cyclohexane has been studied by Kellay *et al* [30], whereas Beysens and Estevé [31] focus on the growth of wetting layers in the mixture H_2O–2,6-lutidine by means of light scattering techniques. Plech *et al* [32–34] employ x-ray reflectivity and diffuse scattering under grazing angles to investigate binary organic mixtures wetting silica and fused-silica surfaces. A particularly interesting experimental study is the work by Sallami *et al* [35], who present evidence for layering transitions in water–2,5-dimethylpyridine (2,5-DMP) mixtures. If one plots the relative adsorption of 2,5-DMP as a function of the mole fraction of the organic compound the resulting adsorption isotherms exhibit discontinuous 'jumps' separated by nearly flat, plateau-like regions. These 'jumps' are fingerprints of layering transitions at the solid surface. The relevance of the study by Sallami *et al* to the present work lies in the fact that the former authors

argue that intermolecular interactions causing the layering transitions in the experimental system may be short-range.

Theoretically, wetting of solid substrates by symmetric binary mixtures has been studied in the past by a number of research groups. Most of these earlier studies are, however, concerned with wetting near liquid–liquid coexistence in the bulk [19, 28, 29, 36–38]. Gas adsorption and wetting behaviour of binary mixtures near gas–liquid coexistence have been analysed by Hadjiagapiou and Evans by means of a (continuous) mean-field density functional approach [39]. Later Schmid and Wilding used Ginzburg–Landau theory and Monte Carlo simulations to investigate the wetting behaviour of binary mixtures at gas–liquid coexistence [40]. More recently, Silbermann *et al* [41] employed a mean-field lattice model similar to the one on which the present study is based to investigate the wetting behaviour of binary wetting films.

In all three studies [39–41] intermolecular interactions are governed by short-range potentials. More specifically, Hadjiagapiou and Evans [39] base their work on the Berthelot mixing rule for the interaction between unlike molecules of both species. Moreover, their mixtures are asymmetric in the sense that the interaction between a pair of like molecules of one mixture component differs from that of the other one. As the temperature changes the morphology of the adsorbed films changes and transitions from partial to complete wetting are found (see figure 3 in [39]). Focusing on mixtures with a moderate tendency towards liquid–liquid phase separation, Schmid and Wilding investigate wetting phenomena as a function of the fluid–substrate attraction ϵ_{W}. In their study T_{w} always exceeds the critical end point (cep) at which critical mixed and demixed liquid phases coexist with a noncritical gaseous phase. Silbermann *et al* [41] showed how the character of the wetting film (i.e., mixed *versus* demixed) changes with substrate selectivity (i.e., the energetic preference of adsorption of molecules of one species by the solid substrate). However, on account of the high dimension of the parameter space on which their model is defined, the study by Silbermann *et al* is restricted to a rather narrow range of system parameters.

In contrast, the present study aims at spanning a much wider range of model parameters. A focal point here is the competition between the tendency towards decomposition of bulk mixtures and (nonselective) adsorption of mixture molecules by the solid substrate. Therefore this work extends the earlier study of Wilding and Schmid in a systematic way by also varying the attraction strength between unlike fluid molecules ϵ_{AB} in addition to ϵ_{W}. As we shall demonstrate below, the interplay between both parameters is of central importance for the phase behaviour and composition of wetting films. For example, as a result of this interplay we observe wetting at *all* temperatures $T \geqslant 0$ for which we have coexisting phases in the bulk. Our results offer the possibility to comprehend why layering may occur for $T < T_{\mathrm{cep}}$ but complete wetting will not.

The remainder of this paper is organized as follows. In section 2 we introduce our model and a mean-field approximation for the intrinsic free-energy functional on which all calculations in this work are predicated. Some elementary thermodynamic concepts are introduced in section 3. Section 4 is devoted to theoretical concepts central to complete wetting. Section 5 is given to a presentation of our results. Our findings are summarized and put into perspective in the concluding section 6.

2. Model and mean-field approximation

2.1. Nearest-neighbour lattice gas

We consider a binary (A–B) mixture on a simple cubic lattice of $\mathcal{N} = nz$ sites, whose lattice constant is ℓ. The position of a fluid molecule on this lattice is specified by a pair of integers

(k, l) where $1 \leqslant k \leqslant n$ labels the position in an x–y plane and $1 \leqslant l \leqslant z$ determines the position of that plane along the z-axis. A specific site may be occupied either by a molecule of species A or B, or it may be altogether empty. To describe individual configurations on the lattice we introduce a matrix $\mathbf{s}$ of occupation numbers such that

$$s_{kl} = \begin{cases} +1, & \text{site occupied by molecule of component A} \\ 0, & \text{empty site} \\ -1, & \text{site occupied by molecule of component B.} \end{cases} \tag{2.1}$$

For given $\mathbf{s}$ the total number of sites occupied by molecules of species A or B is $N_{\mathrm{A}}(\mathbf{s})$ or $N_{\mathrm{B}}(\mathbf{s})$, respectively, for which explicit expressions are derived in (2.2a) and (2.2b) of an earlier paper by Woywod and Schoen [27]. Based upon these expressions Woywod and Schoen also calculated the total number of A–A $[N_{\mathrm{AA}}(\mathbf{s})]$, B–B $[N_{\mathrm{BB}}(\mathbf{s})]$, and A–B nearest-neighbour pairs $[N_{\mathrm{AB}}(\mathbf{s})]$ on the lattice (see (2.6a), (2.6b), and (2.6c) in [27]).

We *formally* confine the mixture by two impenetrable solid substrates located at $l = 0$ and $l = z + 1$ and introduce the number of molecules of type A and B at those substrates, $N_{\mathrm{AW}}(\mathbf{s})$ and B, $N_{\mathrm{BW}}(\mathbf{s})$, respectively (see (2.4) and (2.5) of [27]). In what follows we take $z = 40$–90, which is sufficiently large so that adsorption of molecules at one solid surface is not perturbed by the presence of the other.

In addition, we assume all interactions (i.e., fluid–fluid and fluid–substrate) to be pairwise additive, and model them according to square-well potentials where the width of the attractive well is set equal to the diameter σ of a fluid molecule (taking the same value of σ for both species). Hence, we restrict ourselves exclusively to nearest-neighbour attractions, that is $\ell = \sigma$. The restriction to a maximum occupation of each site by at most one molecule (see (2.1)) accounts for the infinitely hard core imposed by the square-well potential.

The energy function (i.e., the Hamiltonian) governing our system can then be cast as

$$\begin{aligned} \mathcal{H}(\mathbf{s}; \tilde{\mu}) = {} & \epsilon_{\mathrm{AA}}[N_{\mathrm{AA}}(\mathbf{s}) + N_{\mathrm{BB}}(\mathbf{s})] + \epsilon_{\mathrm{AB}} N_{\mathrm{AB}}(\mathbf{s}) + \epsilon_{\mathrm{W}}[N_{\mathrm{AW}}(\mathbf{s}) + N_{\mathrm{BW}}(\mathbf{s})] \\ & - \tilde{\mu}[N_{\mathrm{A}}(\mathbf{s}) + N_{\mathrm{B}}(\mathbf{s})] \end{aligned} \tag{2.2}$$

where $\tilde{\mu}$ is the chemical potential which we deliberately choose to be equal for both mixture components to limit the dimension of the parameter space on which our model is defined, and

$$\epsilon_{\mathrm{AA}} = \epsilon_{\mathrm{BB}} \leqslant \epsilon_{\mathrm{AB}} < 0 \tag{2.3}$$

$$\epsilon_{\mathrm{W}} = \epsilon_{\mathrm{AW}} = \epsilon_{\mathrm{BW}} < 0. \tag{2.4}$$

On account of (2.3), molecules are distinguished solely by their 'colour' such that only the attraction between a pair of differently coloured molecules differs from that between a pair of equally coloured ones. This model mixture is usually referred to as 'symmetric' [42]. If the second equality holds in (2.3), the symmetric binary mixture degenerates into a pure (i.e., one-component) fluid. As in our previous paper [27], we assume the walls to be 'nonselective', that is, from a purely energetic perspective the adsorption of a molecule of species A is indistinguishable from that of a molecule of species B (see (2.4)).

2.2. Lattice-gas Hamiltonian in mean-field approximation

Based upon these considerations we may introduce the partition function Ξ in the grand canonical ensemble via [42]

$$\Xi(\mathcal{N}, T, \tilde{\mu}) = \sum_{\{\mathbf{s}\}} \exp[-\mathcal{H}(\mathbf{s}; \tilde{\mu})/k_{\mathrm{B}}T] \equiv \exp(-\Omega/k_{\mathrm{B}}T) \tag{2.5}$$

where $\Omega(\mathcal{N}, T, \mu)$ is the grand potential. To proceed we introduce a mean-field approximation for the Hamiltonian specified in (2.2). It consists of *assuming* that within each lattice plane l

parallel to the solid substrates the occupation number at each lattice site can be replaced by an *average* occupation number for the *entire* plane. On account of the symmetry-breaking nature of the solid substrate these average occupation numbers will generally vary between planes, that is they will change with l. In this sense our model accounts for correlations in the direction *perpendicular* to the substrate planes but ignores these correlations altogether within each of the z lattice planes *parallel* to the substrates. Hence, we introduce the total *local* density

$$\rho_l = \rho_l^{\mathrm{A}} + \rho_l^{\mathrm{B}} = \frac{1}{n}\sum_{k=1}^{n} s_{kl}^2 \equiv \frac{n_l^{\mathrm{A}} + n_l^{\mathrm{B}}}{n} \equiv \frac{n_l}{n} \tag{2.6}$$

where $0 \leqslant \rho_l \leqslant 1$ in units of σ^3. As a second order parameter we define the *local* 'miscibility' m_l via

$$m_l \rho_l = \rho_l^{\mathrm{A}} - \rho_l^{\mathrm{B}} = \frac{1}{n}\sum_{k=1}^{n} s_{kl} \tag{2.7}$$

as a quantitative measure of the degree of local decomposition of the binary mixture such that $-1 \leqslant m_l \leqslant 1$. For example, if at plane l the fluid consists of pure component A, (2.7) implies $m_l = 1$. Likewise, if at plane l pure component B is present, $m_l = -1$. If, on the other hand, we have perfect miscibility across plane l, $\rho_l^{\mathrm{A}} = \rho_l^{\mathrm{B}}$ (subject to (2.6) and the constraint $\rho_l \leqslant 1$) and hence $m_l = 0$. In other words, the phase behaviour of the binary mixture is characterized by two sets of *local* order parameters, namely $\boldsymbol{\rho} \equiv \{\rho_1, \ldots, \rho_z\}$ and $\boldsymbol{m} \equiv \{m_1, \ldots, m_z\}$, where we note in passing that both ρ_l and m_l are continuous only in the thermodynamic limit $n \to \infty$.

Mathematically speaking, the mean-field approximation consists of mapping the $n \times z$ occupation-number matrix $\mathbf{s}$ onto the z-dimensional vectors $\boldsymbol{\rho}$ and $\boldsymbol{m}$. Hence, we replace $H(\boldsymbol{s}; \tilde{\mu})$ by its mean-field analogue $H_{\mathrm{mf}}(\boldsymbol{\rho}, \boldsymbol{m}; \tilde{\mu})$. An explicit expression for H_{mf} is derived in appendix A of the paper by Silbermann *et al* [41]. To derive the mean-field analogue of (2.5) we follow these authors, who argued that in mean-field approximation one has the expression

$$\omega(T, \tilde{\mu}) = \frac{\Omega_{\mathrm{mf}}}{\mathcal{N}} = -\frac{k_{\mathrm{B}}T}{\mathcal{N}} \ln \Theta(\boldsymbol{\rho}, \boldsymbol{m}) + \frac{\mathcal{H}_{\mathrm{mf}}(\boldsymbol{\rho}, \boldsymbol{m}; \tilde{\mu})}{\mathcal{N}} \tag{2.8}$$

for the grand-potential density $\omega = \Omega/\mathcal{N}$. Explicit forms for both the combinatorial factor Θ and the grand-potential density ω are derived in appendix B of [41]. From the final expression for $\omega(T, \tilde{\mu})$ given in that paper we obtain for the special case of a symmetric mixture interacting with nonselective solid surfaces the equation

$$\begin{aligned}
\omega(T, \tilde{\mu})|_{\rho,m} = {} & \frac{k_{\mathrm{B}}T}{z}\sum_{l=1}^{z}[\rho_l \ln \rho_l + (1-\rho_l)\ln(1-\rho_l) - \rho_l \ln 2] \\
& + \frac{k_{\mathrm{B}}T}{2z}\sum_{l=1}^{z}\rho_l[(1+m_l)\ln(1+m_l) + (1-m_l)\ln(1-m_l)] \\
& + \frac{\epsilon_{\mathrm{AA}}}{4z}\sum_{l=1}^{z}[\rho_l\rho_{l-1}(1+m_l m_{l-1}) + 4\rho_l^2(1+m_l^2) + \rho_l\rho_{l+1}(1+m_l m_{l+1})] \\
& + \frac{\epsilon_{\mathrm{AB}}}{4z}\sum_{l=1}^{z}[\rho_l\rho_{l-1}(1-m_l m_{l-1}) + 4\rho_l^2(1-m_l^2) + \rho_l\rho_{l+1}(1-m_l m_{l+1})] \\
& - \frac{\tilde{\mu}}{z}\sum_{l=1}^{z}\rho_l + \frac{\epsilon_{\mathrm{W}}}{z}(\rho_1 + \rho_z)
\end{aligned} \tag{2.9}$$

where the first two terms on the right-hand side of (2.9) represent the entropic contribution to the intrinsic free-energy functional. The contribution of intermolecular interactions is accounted

for by the third and fourth terms, whereas the fifth one arises because our system is coupled to an (infinitely large) reservoir of matter maintained at fixed $\tilde{\mu}$ and T. The last term in (2.9) stands for the interaction of the (*formally* confined) mixture with two solid substrates located at $l = 1$ and z, respectively. The term proportional to $\rho_l \ln 2$ in (2.9) represents a trivial entropic contribution because molecules of both mixture species can always be distinguished on account of their different 'colour'.

3. Thermodynamic aspects

3.1. Phases and phase equilibrium

Based upon the explicit expression for the grand-potential density given in (2.9) we are now in a position to address the question of phase equilibrium. Generally speaking, the condition for coexistence between any two phases can be stated as

$$\omega^{\alpha}(T, \tilde{\mu}_{\alpha\beta}) = \omega^{\beta}(T, \tilde{\mu}_{\alpha\beta}) \tag{3.1}$$

for a given temperature T, where $\omega^{\alpha}(T, \tilde{\mu}_{\alpha\beta})$ is an abbreviation for the grand-potential density $\omega(T, \tilde{\mu}_{\alpha\beta})|_{\rho^{\alpha}, m^{\alpha}}$ of a specific (globally or meta-) stable configuration (i.e., phase) characterized by $\boldsymbol{\rho}^{\alpha}$ and $\boldsymbol{m}^{\alpha}$ (see below). For fixed temperature, (3.1) determines the chemical potential $\tilde{\mu}_{\alpha\beta}$ at which the phases coexist. Because ω represents a complex energy hyperplane in thermodynamic state space it is conceivable that it has many local minima represented by the set $\{\boldsymbol{\rho}^{i}, \boldsymbol{m}^{i}\}$. Most of the pairs of phases complying with (3.1) are, however, only *metastable* at coexistence. The pair representing the *thermodynamically* stable phases at coexistence is the one satisfying

$$\omega^{\alpha}(T, \tilde{\mu}_{\alpha\beta}) = \min_{\gamma} \omega^{\gamma}(T, \tilde{\mu}_{\alpha\beta}) \tag{3.2}$$

in addition to (3.1).

In general, a range of temperatures exists over which the set $\{\boldsymbol{\rho}^{\alpha}, \boldsymbol{m}^{\alpha}\}$ satisfies equations (3.1) and (3.2) simultaneously. Since both $\tilde{\mu}_{\alpha\beta}, T \in \mathbb{R}$, it will prove convenient to introduce the notion of a line $\tilde{\mu}_{\alpha\beta}(T)$ in thermodynamic state space (i.e., the *coexistence line*) as the set of points $\{\tilde{\mu}_{\alpha\beta}, T\}$ obtained as a solution of (3.1) subject to the constraint posed by (3.2). The coexistence line therefore represents a line of discontinuous (i.e., first-order) phase transitions between phases α and β as long as $\{\boldsymbol{\rho}^{\alpha}, \boldsymbol{m}^{\alpha}\} \neq \{\boldsymbol{\rho}^{\beta}, \boldsymbol{m}^{\beta}\}$, that is as long as the two phases are morphologically different. Moreover, we define as a *phase diagram* the union of all coexistence lines, that is

$$\tilde{\mu}_{x}(T) = \bigcup_{\alpha,\beta} \tilde{\mu}_{\alpha\beta}(T). \tag{3.3}$$

Henceforth we shall use the notation $\tilde{\mu}_{x}^{\infty}(T)$ to distinguish the bulk phase diagram from those where wetting films may form as thermodynamically stable phases on account of the presence of a solid substrate. Several of the phase diagrams presented in this work exhibit isolated points at which

$$\tilde{\mu}_{\mathrm{tri}} = \tilde{\mu}_{\alpha\beta}(T_{\mathrm{tri}}) = \tilde{\mu}_{\beta\gamma}(T_{\mathrm{tri}}) = \tilde{\mu}_{\alpha\gamma}(T_{\mathrm{tri}}) \tag{3.4}$$

holds, describing coexistence between three thermodynamic phases α, β, and γ at a triple point $(\mu_{\mathrm{tri}}, T_{\mathrm{tri}})$.

Because we restrict ourselves to symmetric mixtures, a demixed A-rich phase cannot be distinguished from a demixed B-rich phase. This symmetry is reflected by the symmetry of ω in (2.9) with respect to the transformation $\boldsymbol{m} \longrightarrow -\boldsymbol{m}$. Therefore, the term 'demixed' always refers to a situation where a phase bearing a surplus of one component coexists with

a phase in which the composition is dominated by molecules of the other component. In addition, continuous phase transitions from mixed to demixed phases are critical in the sense that coexistence between the participating (indistinguishable) demixed phases becomes critical. The set of state points for which this is the case may be perceived as a line of critical points, which we refer to as a λ-line in accord with conventional terminology [42].

3.2. Coexisting mixed liquid and gas bulk phases

We begin by applying the above considerations to a situation in which mixed liquid and gas bulk phases coexist. According to section 2.2, and because of the symmetry inherent in our model mixture (see (2.3)), this implies $\boldsymbol{m} = \boldsymbol{0}$ for both phases regardless of T. It is then easy to verify from the expression for the grand-potential density given in (2.9) that

$$\omega(T, \mu) = k_{\mathrm{B}}T[\rho \ln \rho + (1 - \rho)\ln(1 - \rho)] + 3\overline{\epsilon}\rho^2 - \mu\rho \tag{3.5}$$

where

$$\overline{\epsilon} = \frac{\epsilon_{\mathrm{AA}} + \epsilon_{\mathrm{AB}}}{2}. \tag{3.6}$$

Equation (3.5) is derived from (2.9) because in thermodynamic equilibrium and in the absence of external fields (i.e., for $\epsilon_{\mathrm{W}} = 0$) symmetry dictates that all elements of the vector $\boldsymbol{\rho}$ have to assume the same value ρ. In (3.5),

$$\mu = \tilde{\mu} + k_{\mathrm{B}}T \ln 2 \tag{3.7}$$

is an auxiliary chemical potential which we introduce to conveniently eliminate the trivial entropy contribution. From (3.5) it is then straightforward to verify that the critical temperature and chemical potential are given by [43]

$$T_{\mathrm{c}}^{+} = \frac{k_{\mathrm{B}}T_{\mathrm{c}}}{|\overline{\epsilon}|} = \frac{3}{2} \tag{3.8}$$

$$\mu_{\mathrm{c}}^{+} = \frac{\mu_{\mathrm{c}}}{|\overline{\epsilon}|} = -3. \tag{3.9}$$

The coexistence line between *mixed* (M) liquid and gas (G) in the bulk can therefore be mapped onto that between *pure* bulk liquid and gas, where the mean intermolecular attraction between a pair of fluid molecules is given by $\overline{\epsilon}$. Hence, the coexistence line $\mu_{\mathrm{GM}}^{\infty} = -3|\overline{\epsilon}|$ (see table 1) will always be a horizontal line parallel to the T axis. In this sense $\overline{\epsilon}$ determines a sensible 'natural' energy scale for mixed liquid and gas phases. Any deviations of $\mu_{\mathrm{GM}}^{\infty}(T)$ from $-3|\overline{\epsilon}|$ can therefore be attributed to deviations from perfect miscibility of the pure components. Consequently, we shall henceforth express the chemical potential and ϵ_{W} in units of $|\overline{\epsilon}|$; temperature will be cast in units of $|\overline{\epsilon}|/k_{\mathrm{B}}$. We refer to this set as dimensionless (i.e., 'reduced') variables identified by the plus symbol (+). A quantity like ϵ_{AB}, on the other hand, will be expressed in units of $|\epsilon_{\mathrm{AA}}|$ following our previous practice [27, 41]. To distinguish the former set of dimensionless variables from the latter we shall use an asterisk (∗) as superscript for ϵ_{AB} given in units of $|\epsilon_{\mathrm{AA}}|$. From this definition and (3.6) it is easy to verify that the transformation between both energy scales is effected by $x^* \longrightarrow x^+ = fx^*$, where

$$f = \frac{2}{1 + |\epsilon_{\mathrm{AB}}^*|}. \tag{3.10}$$

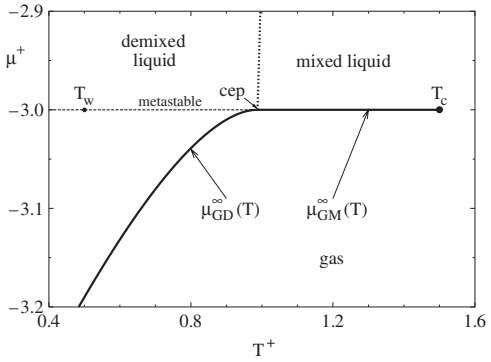

Figure 1. Bulk phase diagram for $|\epsilon^*_{AB}| = 0.70$, where metastable gas-mixed liquid $[\mu^{\infty}_{GM}(T)]$ and gas-demixed liquid coexistence lines $[\mu^{\infty}_{GD}(T)]$ are also indicated; (——) line of discontinuous phase transitions ending at the gas-mixed liquid critical point $\mu^+_c = -3$, $T^+_c = \frac{3}{2}$; $(\cdots)$ (critical) λ-line starting at the critical end point (cep) $\mu^+_{cep} = -3.0$, $T^+_{cep} \simeq 0.99$ and separating mixed and demixed phases through continuous phase transitions. The hypothetical wetting temperature $T_w \simeq 0.5$ (see the text).

Table 1. Notation to identify phases $\mathcal{P}^{\alpha}$.

α	Nature of phase
G	Bulk gas
L	Pure bulk liquid
M	Mixed bulk liquid
D	Demixed bulk liquid
k	Pure film of k layers
mk	Mixed film of k layers
dk	Demixed film of k layers

4. Wetting of solid surfaces

4.1. Phenomenological approach

The discussion in section 3 now enables us to treat wetting and layering phenomena as substrate-induced phase transitions. Intuitively, one thus expects the fluid–substrate attraction to become particularly important. To see the latter let us briefly elaborate on a simple phenomenological argument.

Consider a sessile droplet of liquid on a solid substrate. Its contact angle θ is determined by the Young–Dupré equation [44]

$$\cos\theta = \frac{\sigma_{gs} - \sigma_{ls}}{\sigma_{gl}} \tag{4.1}$$

where σ_{ij} is the interfacial tension between gas (g), liquid (l), and solid (s) phases (see figure 1(a)).

To obtain a rough estimate for the set $\{\sigma_{ij}\}$, simple heuristic energetic arguments may be invoked. Consider the following *Gedanken experiment* by which we introduce an auxiliary plane in a hypothetical, infinitely large body of liquid without interfaces. We then remove that portion of liquid above the plane. This creates a liquid–gas interface by breaking 'bonds' (i.e., cutting off interactions) between molecules across the newly formed interface. As a result the

free energy of the now semi-infinite remainder of liquid will increase by an amount

$$\sigma_{\mathrm{gl}} \simeq \tfrac{1}{2}\rho_{\mathrm{liq}}^2\epsilon_{\mathrm{liq}} \tag{4.2}$$

for sufficiently low temperatures where one may safely assume entropic contributions to be negligible. In (4.2), ρ_{liq} is the density in the semi-infinite liquid slab and ϵ_{liq} is a measure of the strength of attraction between a pair of liquid molecules. Note that no distinction is being made between pure fluids and (multicomponent) mixtures.

To create a solid–liquid interface we proceed as before, that is we introduce a second auxiliary plane in the liquid, and remove the portion of liquid *below* that plane, but this time replace it by solid which, in turn, lowers the (free) energy by approximately $\rho_{\mathrm{liq}}\epsilon_{\mathrm{W}}$. Thus,

$$\sigma_{\mathrm{ls}} \simeq \tfrac{1}{2}\rho_{\mathrm{liq}}^2\epsilon_{\mathrm{liq}} - \rho_{\mathrm{liq}}\epsilon_{\mathrm{W}}. \tag{4.3}$$

For sufficiently low temperatures it seems fair to assume that the density of the gas phase essentially vanishes. Hence,

$$\sigma_{\mathrm{gs}} \simeq 0. \tag{4.4}$$

With the aid of equations (4.2)–(4.4) one obtains from (4.1)

$$\cos\theta \simeq \frac{2}{\rho_{\mathrm{liq}}}\frac{\epsilon_{\mathrm{W}}}{\epsilon_{\mathrm{liq}}} - 1. \tag{4.5}$$

Hence, from (4.5) we expect complete wetting (i.e., $\cos\theta = 1$) to occur if

$$\epsilon_{\mathrm{W}} \leqslant \rho_{\mathrm{liq}}\epsilon_{\mathrm{liq}} < 0, \tag{4.6}$$

that is complete wetting depends crucially on the relative strengths of fluid–fluid and fluid–substrate attraction (see section 5.1).

4.2. The limit of vanishing temperature

4.2.1. Bulk phases. In the limit of vanishing temperature (i.e., for $T = 0$), (2.9) permits us to substantiate (4.6) since phase equilibria can be treated analytically. As we already showed in section 3.2, $\overline{\epsilon}$ may be viewed as a natural energy unit for the coexistence between mixed liquid and gas bulk phases (see table 1). Unfortunately, this is not so for the coexistence between demixed liquid (D) and gas bulk phases. The simple reason is that for a demixed liquid $\boldsymbol{m} \neq \mathbf{0}$. However, since one is still dealing with the bulk, symmetry still dictates that $\boldsymbol{m}$ can be replaced by z times a single value m which simplifies the treatment of ω in (2.9) somewhat. However, m depends on the thermodynamic state such that $\mu_{\mathrm{GD}}^{\infty}(T)$ (see table 1) is not constant like $\mu_{\mathrm{GM}}^{\infty}(T)$ but depends in an *a priori* unpredictable manner on T. Fortunately, some insight can still be gained in the limit $T = 0$ where $\rho = 0, 1$ and $m = \pm 1$, thus enabling an analytic solution of (3.1) for various pairs of coexisting phases.

We begin with coexisting gaseous and demixed liquid phases. From (2.9) and (3.1) we obtain

$$\omega^{\mathrm{G}} = 0 = -\mu_{\mathrm{GD}} + 3\epsilon_{\mathrm{AA}} = \omega^{\mathrm{D}}(\mu_{\mathrm{GD}}) \tag{4.7}$$

from which $\mu_{\mathrm{GD}}^{*} = -3$ follows without further ado. In (4.7) we dropped the argument $T = 0$ and realized that in this limit $\tilde{\mu} = \mu$ (see (3.7)). In (4.7) we also used the fact that, for $T = 0$, the density of the gas phase vanishes, and hence $\omega^{\mathrm{G}} = 0$. It is instructive to convert μ_{GD} to units of $|\overline{\epsilon}|$, that is to 'natural' units of μ_{GM}. With the aid of (3.6) we readily obtain

$$\mu_{\mathrm{GD}}^{+} = \frac{2\mu_{\mathrm{GD}}^{*}}{1 + |\epsilon_{\mathrm{AB}}^{*}|} = -\frac{6}{1 + |\epsilon_{\mathrm{AB}}^{*}|}, \tag{4.8}$$

that is for $T = 0$ and $|\epsilon^*_{AB}| \leqslant 1$,

$$\mu^+_{GD} \leqslant \mu^+_{GM} = -3 \tag{4.9}$$

where the equality holds if the binary mixture degenerates into a pure liquid where all interactions are the same (i.e., $\epsilon_{AA} = \epsilon_{BB} = \epsilon_{AB}$). Therefore, for $|\epsilon^*_{AB}| < 1$ gas always coexists with a demixed liquid phase, rendering the mixed phase metastable.

4.2.2. Wetting films. Turning now to a microscopic treatment of thin films adsorbed on a solid substrate we focus first on coexistence between gas and mixed monolayer film. For a monolayer film $z = 1$, $\rho_1 = 1$ and $\rho_0 = \rho_2 = 0$. From (2.9) we therefore have

$$\omega^{m1}(\mu) = \epsilon_{AA} + \epsilon_{AB} + \epsilon_W - \mu \tag{4.10}$$

which follows because for a mixed monolayer film at $T = 0$, $\rho_1 = 1$ and $m_1 = 0$. Therefore, the previous expression gives ($\omega^G = 0$)

$$\mu^+_{Gm1} = -\frac{2(1 + |\epsilon^*_{AB}| + |\epsilon^*_W|)}{1 + |\epsilon^*_{AB}|} \tag{4.11}$$

where we also employed equations (3.1) and (3.6). Similar reasoning for a demixed monolayer film where $m_1 = \pm 1$ gives

$$\mu^+_{Gd1} = -\frac{2(2 + |\epsilon^*_W|)}{1 + |\epsilon^*_{AB}|}, \tag{4.12}$$

that is for $T = 0$ we are effectively dealing with a pure monolayer film composed entirely of molecules of either species because

$$\mu^+_{Gd1} \leqslant \mu^+_{Gm1} \tag{4.13}$$

where the equality holds for $|\epsilon^*_{AB}| = 1$, that is if the binary monolayer mixture degenerates (formally) into a pure phase.

Turning now to coexistence between mixed films comprising k and $k' = k + 1$ layers, respectively, we obtain from (2.9)

$$\omega^{mk}(\mu) = \frac{\overline{\epsilon}}{z}(3k - 1) - \frac{\mu}{z} + \frac{\epsilon_W}{z}. \tag{4.14}$$

Changing $k \to k'$ in this last expression and invoking again (3.1) we obtain for the chemical potential at coexistence between these films

$$\mu^+_{mkmk'} = -3 \tag{4.15}$$

which is not only independent of the presence of a solid substrate but resembles precisely μ^+_{GM}. We are thus confronted with a situation where the solid substrate has no influence on the phase equilibrium between thicker films, whereas by altering ϵ_{AA} or ϵ_W, μ_{Gm1} can be shifted at our demand (see (4.11)). This implies that for $T = 0$ a one-phase region for mixed monolayer films exists whose width can be altered by changing ϵ_{AB} and/or ϵ_W. The fact that only the gas-mixed monolayer phase coexistence depends on ϵ_W is, of course, a feature caused by the short-range character of the fluid–substrate potential governing our model. However, (4.11) and (4.15), together with the analysis put forth in section 3.2, lead us to conclude that for $T = 0$ complete wetting by a macroscopically thick mixed film would be possible *in principle*.

Consider next the situation in which *demixed* films of k and $k' = k + 1$ layers coexist. A straightforward calculation along the lines of the above analysis eventually yields

$$\mu^+_{dkdk'} = -\frac{6}{1 + |\epsilon^*_{AB}|}. \tag{4.16}$$

Comparison of this last expression with (4.15) shows that one can promote coexistence between *demixed* films of k and $k+1$ layers relative to equally thick *mixed* ones by lowering $|\epsilon_{AB}|$. For reasons given above $\mu_{dkdk'}$ turns out to be independent of ϵ_W for $T = 0$.

From (4.15) and (4.16) we thus obtain

$$\mu^{+}_{dkdk'} \leqslant \mu^{+}_{mkmk'} \tag{4.17}$$

where the equality again holds for the limiting case of a pure fluid, that is for $|\epsilon^{*}_{AB}| = 1$. Equation (4.17) leads us to conclude that for $T = 0$ complete wetting occurs where, however, the wetting film is *demixed* rather than *mixed*, the latter being always metastable regardless of its thickness. Comparison of equations (4.13) and (4.17) also indicates that for $T = 0$ gas coexists with an infinite number of progressively thicker demixed films and a demixed bulk phase. Thus, the point $T = 0$, $\mu^{+} = -6/(1 + |\epsilon^{*}_{AB}|)$ constitutes a multiphase point [23].

4.3. Scaling laws

Consider now a symmetric binary mixture where, for example, $|\epsilon^{*}_{AB}| = 0.7$. Because of this choice of ϵ_{AB} the mixture exhibits a moderate tendency towards liquid–liquid phase separation. In other words, for suitably chosen thermodynamic states mixed and demixed phases may arise in addition to a gaseous phase. A typical bulk phase diagram is presented in figure 1. It reveals that for temperatures above that of the critical end point (cep), the bulk phase diagram is indistinguishable from that of a pure fluid apart from the *effective* depth $\overline{\epsilon}$ of the attractive well (see (3.6) and discussion in section 4.2). Hence, the mixture has a *hypothetical* wetting temperature T_w which, for a suitable fluid–substrate attraction, equals that of a corresponding pure fluid (in units of $\overline{\epsilon}$) as shown in figure 1. The wetting temperature is hypothetical because for $T < T_{cep}$, $\mu^{\infty}_{GM}(T) > \mu^{\infty}_{GD}(T)$, and therefore mixed bulk phases are metastable with respect to demixed ones.

It is then instructive to consider the growth of wetting films along $\mu^{\infty}_{x}(T)$ as $T \to T^{-}_{cep}$. In the immediate vicinity of the critical end point useful scaling laws have been derived for the growth of wetting films from which a number of interesting conclusions may be drawn concerning the physical nature of these films. For the subsequent discussion it is therefore sensible to introduce

$$\Delta\mu(\tau) = \mu^{\infty}_{x}(\tau) - \mu_{cep} \tag{4.18}$$

$$\tau = \frac{T_{cep} - T}{T_{cep}}. \tag{4.19}$$

As one approaches the critical end point along the coexistence line $\mu^{\infty}_{GD}(\tau)$ (see figure 1) the thickness l of an adsorbed film will diverge logarithmically, that is [5, 6]

$$l(\Delta\mu, \tau) \propto -\ln[\Delta\mu(\tau)]. \tag{4.20}$$

However, along the coexistence line and in the immediate vicinity of the critical end point one also has [45–48]

$$\Delta\mu \propto \tau^{2-\alpha} \tag{4.21}$$

where α is the relevant critical exponent and therefore (see equations (4.20), (4.21))

$$l(\tau) \propto -\ln\tau. \tag{4.22}$$

Hence, the thickness of the adsorbed film remains finite for all $T < T_{cep}$ and diverges comparably weakly as $\tau \to 0^{+}$. Upon approaching the critical end point (i.e., as $\tau \to 0^{+}$ along $\mu^{\infty}_{x}(T)$) the correlation length of composition fluctuations ξ_{comp}, on the other hand, diverges much faster according to

$$\xi_{comp} \propto \tau^{-\nu}. \tag{4.23}$$

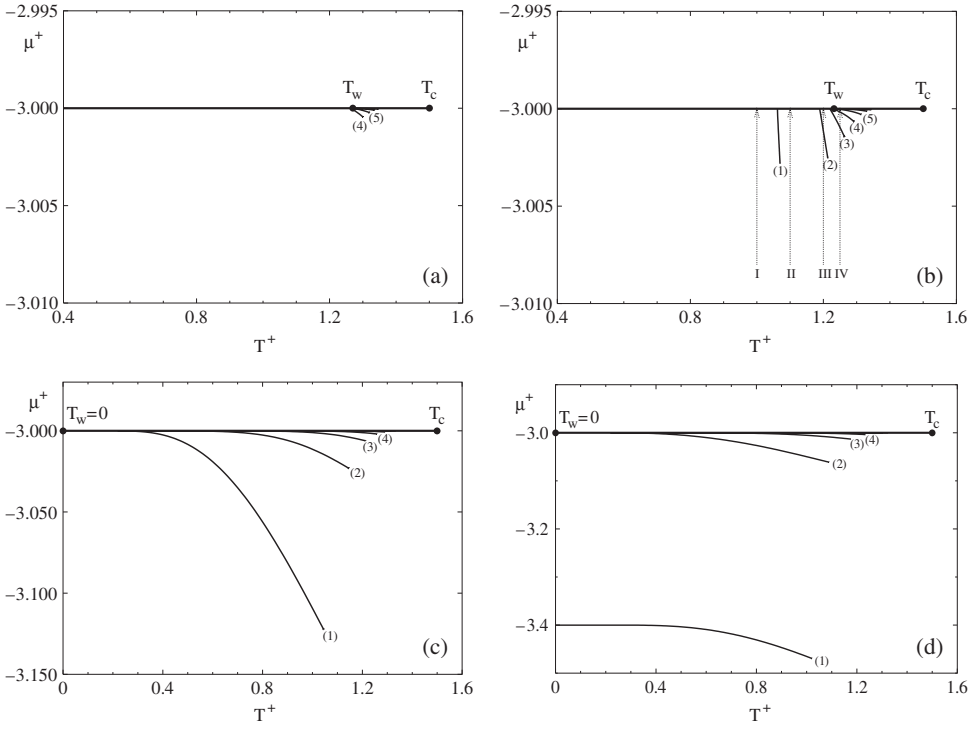

Figure 2. Phase diagrams for $|\epsilon^*_{\mathrm{AB}}| = 1.0$. The numbers ($n$) indicate coexistence lines between films of $n-1$ and n layers where $n-1=0 \mathrel{\hat{=}} \mathrm{G}$ (see table 1). (a) $|\epsilon^+_{\mathrm{W}}| = 0.82$. (b) $|\epsilon^+_{\mathrm{W}}| = 0.84$; vertical dashed lines represent isotherms for which the excess coverage is plotted in figure 3. (c) $|\epsilon^+_{\mathrm{W}}| = 1.00$; in this case $T^+_{\mathrm{w}} = 0$. (d) $|\epsilon^*_{\mathrm{W}}| = 1.40$. In the bulk, gas is thermodynamically stable for $\mu^+ < \mu_x^{\infty+} = -3$, $T^+ \lesssim T_{\mathrm{c}} = \frac{3}{2}$. If, for this temperature range, $\mu > \mu_x^{\infty}$ then the liquid is thermodynamically stable.

Therefore, a range of temperatures $T' \leqslant T \lesssim T_{\mathrm{cep}}$ exists such that $\xi_{\mathrm{comp}} \geqslant l(\tau)$ along $\mu_x^{\infty}(T)$, where the equality holds for $T = T'$. In other words, the size of A- or B-rich domains forming side by side becomes much larger than the actual thickness of the adsorbed film for $T \lesssim T_{\mathrm{cep}}$. This, in turn, implies that along $\mu^{\infty}_{\mathrm{GD}}(T)$ adsorbed films always become mixed *prior* to the bulk critical end point.

However, the above analysis bears an ostensible contradiction. On account of the scaling relation (4.22), $T_{\mathrm{w}} \geqslant T_{\mathrm{cep}}$ because the film thickness diverges to infinity at the critical end point (and, of course, for all higher temperatures at bulk phase coexistence). On the other hand, the discussion in section 4.2 provided clear evidence for complete wetting at $T = T_{\mathrm{w}} = 0$. In this regard a key is that for $T = 0$ the solid surface is wet by a *demixed* liquid phase whereas the scaling prediction implies formation of *mixed* film phases for $T \lesssim T_{\mathrm{cep}}$ along the coexistence line. We shall return to this point in section 5.2.3 below.

5. Results

5.1. Pure fluids

It is instructive to begin a more detailed discussion with pure fluids which are realized for $|\epsilon^*_{\mathrm{AB}}| = 1$. Consider first a relatively weak fluid–substrate attraction of $|\epsilon^*_{\mathrm{W}}| = 0.82$. The plots in figure 2(a) show the gas–liquid coexistence line $\mu^{\infty+}_{\mathrm{GL}} = -3$ ending at the critical

point whose temperature $T_c^+ = \frac{3}{2}$. In addition, films of more than four layers turn out to be thermodynamically stable, as one can see from the plot in figure 2(a). The coexistence lines between films of $n-1$ and n layers start at a layering temperature $T_l(n)$ and end at a layering critical temperature $T_{lc}(n)$, both of which depend on the number of layers n. In terms of the layering temperature, the wetting temperature T_w may then be defined as the temperature at which an adsorbed film becomes macroscopically thick, that is

$$T_w = \lim_{n\to\infty} T_l(n). \tag{5.1}$$

For the special case $|\epsilon^*_{AB}| = 0.82$ the plot in figure 2(a) shows that the T_l are almost independent of n, that is all coexistence lines start at nearly the same temperature and are fairly short.

This picture changes if $|\epsilon^+_W|$ increases slightly, as figure 2(b) reveals. Additional coexistence lines for mono-, bi-, and trilayer phases arise. One also notices from the plot in figure 2(b) that the shift between neighbouring layering temperatures $\Delta T_l(n) \equiv T_l(n+1) - T_l(n)$ rapidly diminishes with increasing n so that the limit in (5.1) is expected to exist. In addition, $T_{lc}(n)$ increases with n, where the roughening temperature is defined as

$$T_r = \lim_{n\to\infty} T_{lc}(n). \tag{5.2}$$

As one approaches T_r, fluctuations of film thickness grow enormously such that the film–gas interface becomes 'rough' in the sense that individual layers parallel to the solid surface can no longer be discerned.

In our model $T_r = T_c$ and hence $T_w < T_c$, so that we indeed observe layering transitions and complete wetting according to the assertions by Binder and Landau (see the middle plot in figure 2 in [23]). These same authors point out that prewetting (i.e., coexistence between molecularly thin and thick films) can be observed only if $T_r < T_w$. On account of short-range fluid–substrate interactions this latter inequality does not hold for our model. Thus, our model does not allow for prewetting transitions due to the somewhat unrealistic fluid–substrate interactions. However, prewetting transitions are of no concern here.

Nevertheless, our model mimics correctly both partial and complete wetting scenarios as well as layering transitions. This becomes particularly apparent in plots of the excess coverage Γ defined as

$$\Gamma = \int_0^\infty \mathrm{d}z' \, [\rho(z') - \rho_{bulk}] = \ell \sum_{k=1}^{z} \rho_k - \ell z \rho_{bulk} \approx \rho_{liq} l \tag{5.3}$$

plotted in figure 3, where $\rho_{bulk}(T, \mu)$ is the bulk gas density for a given T and μ. Equation (5.3) reflects the discrete nature of our model and shows that Γ is proportional to the thickness l of the adsorbed film. Hence, Γ is of the order of k for adsorbed films comprising k molecular layers, weighted, however, by the mean density of the adsorbed film ρ_{liq}. In figure 3, Γ is calculated as a function of chemical potential for four isotherms identified in figure 2(b). For the path labelled I in figure 2(b), Γ in figure 3 exhibits only a weak dependence on μ up to bulk gas–liquid coexistence (i.e., $\mu - \mu_x^\infty = 0$). The excess coverage remains below 1, indicating that we have submonolayer coverage of the solid surface up to bulk gas–liquid coexistence (i.e., for $\mu - \mu_x^\infty(T_I) \to 0^-$). Similarly, for the path labelled II, Γ depends only weakly on μ. However, the final value of Γ at $\mu - \mu_x^\infty(T_{II}) \simeq 0$ is closer to 1, indicating that a monolayer forms on the substrate, as one would expect from the plot in figure 2(b). Since isotherm II does not intersect the coexistence line $\mu_{G1}(T)$ (see table 1) in figure 2(b), Γ is a continuous function of μ.

If, on the other hand, an isotherm intersects one of the layering coexistence lines in figure 2(b), Γ exhibits a discontinuity. For example, along the path labelled III in figure 2(b), $\mu_{G2}(T)$ is crossed by the isotherm. Consequently, Γ changes discontinuously but remains

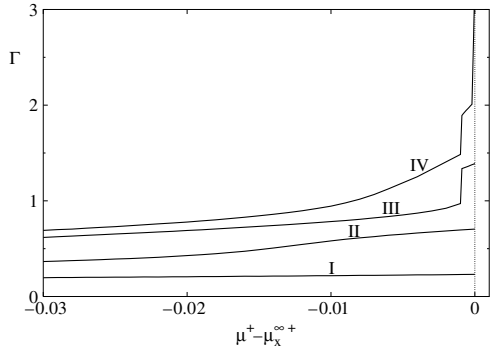

Figure 3. Excess coverage Γ (see (5.3)) as a function of the chemical potential μ relative to the chemical potential at bulk gas–liquid coexistence $\mu_x^{\infty+}$ along the isotherms I–IV identified in figure 2(b).

finite up to bulk gas–liquid coexistence. The terminal value $\Gamma \simeq 1.4$ in figure 3 reflects adsorption of an imperfect bilayer film (i.e., $1 < l\rho_{\mathrm{liq}} < 2$). All three isotherms, I, II, and III, comport with partial wetting.

Complete wetting, on the other hand, is observed along isotherm IV in figure 2(b), where the temperature exceeds T_{w}. Again a layering transition occurs, first reflected by the discontinuity in Γ at $\mu^+ - \mu_x^{\infty+} \simeq 10^{-3}$ in figure 3 followed by a divergence of Γ to infinity as one approaches the bulk coexistence line, that is for $\mu - \mu_x^{\infty} \to 0^-$. However, figure 2(b) reveals that path IV is supercritical with respect to both $T_{\mathrm{lc}}(2)$ and $T_{\mathrm{lc}}(3)$. The continuous but rather pronounced increase of Γ for chemical potentials below $\mu^+ - \mu_x^{+\infty} \simeq 9 \times 10^{-4}$, where the first layering transition arises, reflects this supercriticality. Similar effects have also been observed in pure fluids, as one can see in figure 1(b) of the work by Ball and Evans [38].

If the fluid–substrate attraction increases further, $T_{\mathrm{w}} \to 0$, as the plot for $|\epsilon_{\mathrm{W}}^+| = 1.0$ in figure 2(c) shows. Layering coexistence lines now start at $T = T_{\mathrm{w}} = 0$, and one-phase regions of adsorbed films widen considerably at least for mono- and bilayer films. Further increase of $|\epsilon_{\mathrm{W}}|$ causes the coexistence line for the monolayer film to become detached from the bulk coexistence line. For example, for $|\epsilon_{\mathrm{W}}^+| = 1.4$, $\mu_{\mathrm{G1}}^+(0) \simeq -3.4$, whereas $\mu_{kk'}^+(0) = -3.0$ for $k \geqslant 1$ ($k' = k + 1$) regardless of the magnitude of ϵ_{W}. This effect is only observed for monolayer films, as reflected by equations (4.11) and (4.15). However, we emphasize that $T_{\mathrm{w}} = 0$ for $|\epsilon_{\mathrm{AB}}^*| = 1.0$ is predicted by the phenomenological expression (4.6) because in the limit $T = 0$, $\rho_{\mathrm{liq}} = 1$, and hence complete wetting should occur for all temperatures $0 \leqslant T \leqslant T_{\mathrm{c}}$ if $\epsilon_{\mathrm{W}} \leqslant \epsilon_{\mathrm{liq}} = \epsilon_{\mathrm{AB}}$ (see figure 2(c)). The vanishing of the wetting temperature in the limit of sufficiently attractive solid substrates has also been reported by Binder and Landau (see the uppermost plot in figure 2 of [23]).

5.2. Binary mixtures

5.2.1. The case $|\epsilon_{\mathrm{AB}}^*| = 0.7$. To study the wetting of solid surfaces by binary mixtures we performed a sequence of calculations in which we investigate the wetting of a solid substrate as a function of both ϵ_{AB} and ϵ_{W}. We begin with a mixture for which $|\epsilon_{\mathrm{AB}}^*| = 0.7$ as before, and plot $\mu_x(T)$ for $|\epsilon_{\mathrm{W}}^+| = 0.84$ in figure 4(a).

For this system, $T_{\mathrm{w}} > T_{\mathrm{cep}}$ according to the definition of T_{w} given in (5.1), and the layering coexistence lines for one to three layers are fairly short. In figure 4(a) a number of isotherms I–III are identified for which Γ is plotted in figure 5(a). As expected, Γ is small and depends

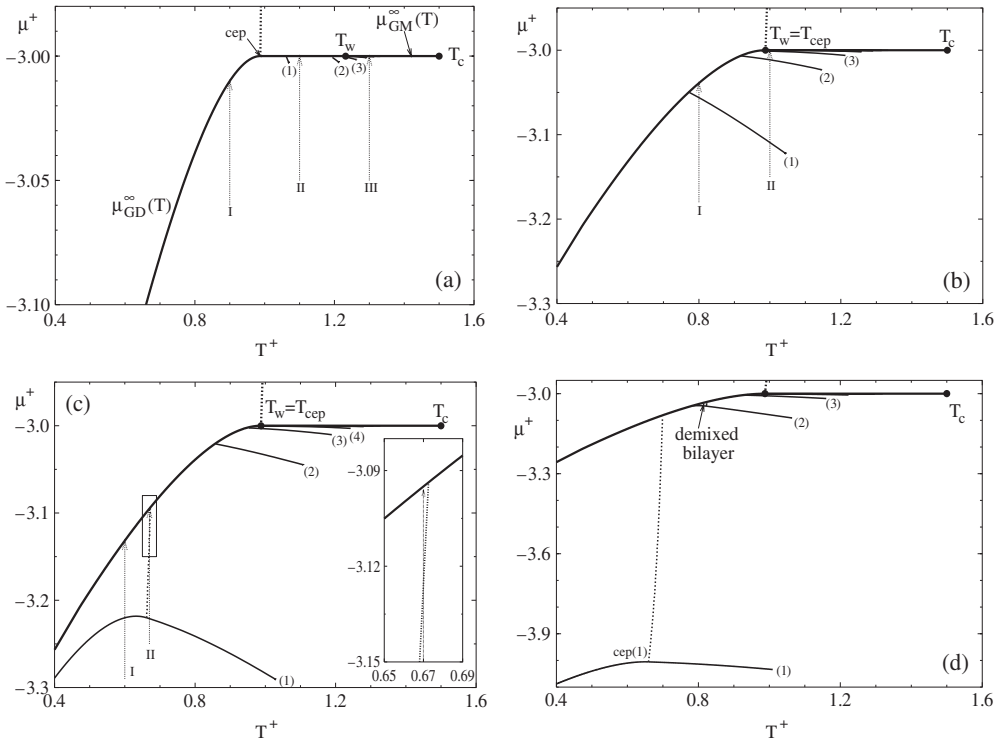

Figure 4. As figure 2 but for $|\epsilon^{*}_{AB}| = 0.7$. (a) $|\epsilon^{+}_{W}| = 0.84$; (b) $|\epsilon^{+}_{W}| = 1.00$; (c) $|\epsilon^{+}_{W}| = 1.20$, where the inset is an enlargement of that portion of the figure bounded by a rectangle; (d) $|\epsilon^{+}_{W}| = 2.00$, where the dotted line represents the surface λ-line starting at $T^{+}_{cep}(1) \simeq 0.66$, $\mu^{+}_{cep}(1) \simeq -3.22$ separating demixed from mixed monolayer films. Note the different scales used on the abscissae of (a)–(d).

only weakly on μ as far as isotherm I is concerned. As before in figure 3 we observe only submonolayer coverage along the isotherm T_I when $\mu_{GD}(T)$ is approached. This is because we are at a temperature below T_w *and* $T_{lc}(1)$. The path labelled II in figure 4(a), on the other hand, approaches $\mu^{\infty}_{x}(T)$ along an isotherm above $T_{lc}(1)$. Therefore, the corresponding plot of Γ in figure 5(a) exhibits a somewhat more pronounced increase with increasing μ, especially close to bulk gas–liquid coexistence (i.e., for $-0.02 < \mu^{+} - \mu^{\infty +}_{x}(T) \lesssim 0$). However, along paths I and II, Γ remains continuous and finite until one reaches bulk gas–liquid coexistence. Therefore, these isotherms comport with a partial wetting scenario.

This situation changes along path III in figure 4(a), where the temperature of the isotherm exceeds T_w. In addition, layering coexistence lines coincide approximately with $\mu^{\infty}_{x}(T)$ for films accommodating four or more layers over the range $T_w \leqslant T \leqslant T_c$. Therefore, Γ in figure 5(a) is a monotonic function of μ diverging at bulk gas–liquid coexistence, that is in the limit $\mu - \mu^{\infty}_{x}(T_{III}) \to 0$. Since this divergence may be interpreted as the formation of a macroscopically thick film, path III in figure 4(a) corresponds to a complete wetting scenario.

Turning now to a more attractive substrate, a plot of $\mu^{\infty}_{x}(T)$ in figure 4(b) shows that $T_w = T_{cep}$ for $\epsilon^{+}_{W} = 1.0$, as predicted by the scaling arguments of section 4.3. Coexistence lines for films comprising between one and four layers also shown in that figure illustrate that for the same number of layers the coexistence lines are significantly longer here compared with their counterparts plotted in figure 4(a). We consider two isotherms labelled I and II in figure 4(b).

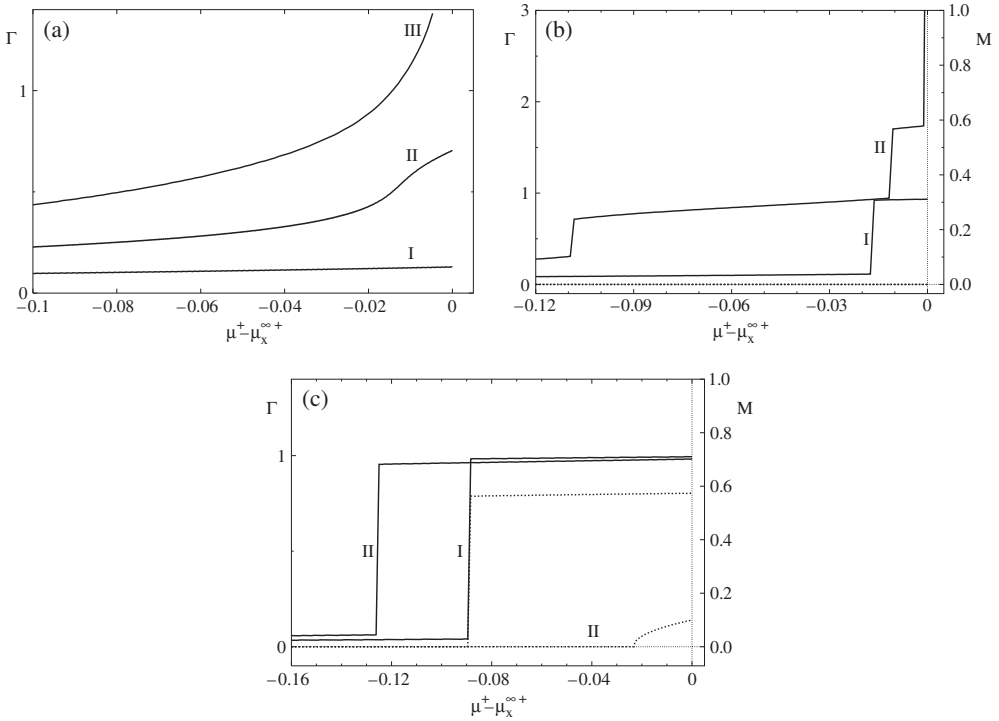

Figure 5. Excess coverage Γ (solid lines, left ordinate) as a function of $\mu^+ - \mu_x^{\infty+}$ and effective miscibility M (see (5.4), dotted lines, right ordinate) for isotherms identified by roman numerals in the corresponding plots of figures 4(a)–(c).

The one labelled I is characterized by $T_{\mathrm{I}} < T_{\mathrm{w}}$, whereas the one labelled II approaches $\mu_x^{\infty}(T)$ along a temperature slightly above T_{w}. Isotherm I intersects $\mu_{\mathrm{G}m1}(T)$. Consequently, the parallel plot of Γ in figure 5(b) exhibits a discontinuity at $\mu - \mu_x^{\infty}(T) \simeq -0.016$. Since $T_{\mathrm{I}} < T_{\mathrm{w}}$, we observe only partial wetting, that is Γ remains finite until we reach bulk gas–liquid coexistence. Isotherm T_{II}, on the other hand, crosses $\mu_{\mathrm{m}k\mathrm{m}k'}(T)$ for $k = 1, 2k' = k + 1$ along T_{II}. The corresponding plot of Γ in figure 5(b) thus exhibits two discontinuities at $\mu^+ - \mu_x^{\infty+}(T) \simeq -0.108$ and -0.011 referring to layering transitions, and then diverges as $\mu - \mu_x^{\infty}(T) \to 0^-$ according to a complete wetting scenario because $T_{\mathrm{II}} > T_{\mathrm{w}}$ such that an infinite number of layering coexistence lines is crossed by the isotherm. That the films are, in fact, mixed is revealed by $M = 0$ up to bulk gas–(mixed) liquid coexistence, where $M \in [-1, 1]$ is a density-independent measure of decomposition of adsorbed films, that is

$$\begin{aligned} M &= \frac{1}{\Gamma}\int_0^{\infty} \mathrm{d}z' \,[\{\rho^{\mathrm{A}}(z') - \rho^{\mathrm{A}}_{\mathrm{bulk}}\} - \{\rho^{\mathrm{B}}(z') - \rho^{\mathrm{B}}_{\mathrm{bulk}}\}] \\ &= \frac{\ell}{\Gamma}\sum_{k=1}^{z}[\rho_k^{\mathrm{A}} - \rho_k^{\mathrm{B}}] - \frac{z\ell}{\Gamma}[\rho^{\mathrm{A}}_{\mathrm{bulk}} - \rho^{\mathrm{B}}_{\mathrm{bulk}}] \end{aligned} \tag{5.4}$$

where Γ is given by (5.3) [41]. Similar to m_l defined in (2.7), $M < 0$, if the adsorbed film is B-rich, whereas it is A-rich if $M > 0$ in the sense of the discussion in section 3.1.

If $|\epsilon_{\mathrm{W}}|$ increases further, the plots in figure 4(c) reveal another change in the overall phase behaviour. For example, if μ is sufficiently low, monolayer films may form which are either mixed or demixed, the two being separated by a λ-line starting at a surface critical end

point for which $T_{\rm cep}^{+} \simeq 0.66$ and $\mu_{\rm cep}^{+} \simeq -3.22$. Considering the isothermal path labelled I in figure 4(c), the parallel plots of Γ in figure 5(c) indicate a layering transition between gas and monolayer phases at $\mu^{+} - \mu_{x}^{\infty +}(T_{\rm I}) \simeq -0.088$. The corresponding plot of the effective miscibility M also shown in figure 5(c) reveals that the newly formed monolayer is demixed because $M \simeq 0.56$ after the phase transition occurred. Along the isotherm $T_{\rm II}$ we first have a layering transition from gas to monolayer for a more negative chemical potential $\mu^{+} - \mu_{x}^{\infty +}(T_{\rm I}) \simeq -0.125$. However, this time the newly formed monolayer is mixed, as reflected by $M = 0$ in figure 5(c). As one continues to move to more positive chemical potentials along the isotherm $T_{\rm II}$ one eventually crosses the surface λ-line separating mixed from demixed monolayer films (see the inset in figure 4(c)). During this continuous phase transition the thickness of the adsorbed film does not change appreciably, as one can see from figure 4(c), where $\Gamma \simeq 0.98 \approx$ constant for $\mu^{+} - \mu_{x}^{\infty +}(T_{\rm II}) \gtrsim -0.022$ along path II. However, as one crosses the λ-line, M rises to more positive values, indicating that the monolayer now becomes (weakly) demixed (see figure 5(c)). Initially, when the isotherm $T_{\rm II}$ intersects the λ-line in figure 4(c),

$$\left.\frac{{\rm d}\mu}{{\rm d}M}\right|_{T=T_{\rm II}} = 0 \tag{5.5}$$

as one would expect for the change of an order parameter at a continuous phase transition. However, both isotherms correspond to partial wetting conditions because Γ remains finite all the way down to $\mu - \mu_{x}^{\infty}(T) \to 0$. If $|\epsilon_{\rm W}|$ reaches a sufficiently large value, this general scenario does not change significantly except for bilayer films, which also appear as mixed and demixed phases (see figure 4(d)). We shall return to this issue shortly in the subsequent section 5.2.2, and refrain from presenting any plots at this point in the interests of brevity.

5.2.2. The case $|\epsilon_{\rm AB}^{*}| = 0.5$. If we lower the attraction strength between a pair of unlike molecules to $|\epsilon_{\rm AB}^{*}| = 0.5$, the topology of $\mu_{x}^{\infty}(T)$ changes completely from the case $|\epsilon_{\rm AB}^{*}| = 0.7$ for which the bulk phase diagram is displayed in figure 4. The most significant change is that for $|\epsilon_{\rm AB}^{*}| = 0.5$ mixed and demixed liquid phases are separated by a coexistence line $\mu_{\rm DM}(T)$ instead of a λ-line (see figure 6). As a consequence the critical end point visible in figure 4 has been transformed into a triple point at which $\mu_{x}^{\infty}(T)$ in figure 6 bifurcates into $\mu_{\rm DM}(T)$ and $\mu_{\rm GM}(T)$. Therefore, both demixed and mixed liquid phases coexist with a gaseous phase at a quadruple point. The temperature of the quadruple point coincides with the wetting temperature $T_{\rm w}$ in the present case.

For $|\epsilon_{\rm W}^{+}| = 1.3$ the plot in figure 6(a) shows that the one-phase region of a demixed monolayer is triangular shaped and enclosed by various other coexistence lines. Let us again consider two isothermal paths labelled I and II in figure 6(a). Along $T_{\rm I}$ we cross $\mu_{Gd1}(T)$ before eventually reaching the bulk coexistence line. Consequently, the parallel plot of Γ in figure 7 exhibits a single discontinuity at $\mu^{+} - \mu_{x}^{\infty +}(T_{\rm I}) \simeq -0.024$. At $\mu^{+} - \mu_{x}^{\infty +}(T_{\rm I}) \simeq -0.024$, M, too, exhibits a discontinuous change and increases to $M \simeq 0.79$, indicating that a demixed monolayer has formed. Along path II (see figure 6(a)) two coexistence lines are crossed. At the first intersection at $\mu^{+} - \mu_{x}^{\infty +}(T) \simeq -0.066$, Γ changes discontinuously to a value of about $\Gamma \simeq 0.64$. As μ increases further Γ keeps rising, too. However, eventually a second discontinuity at $\mu^{+} - \mu_{x}^{\infty +}(T) \simeq -0.031$ is observed, at which Γ assumes a value of about 0.87. Hence, the initial monolayer film becomes a bit denser. Between the first and second discontinuity $M = 0$, indicating that the monolayer film is mixed. At the second discontinuity, however, M rises to a value of about 0.53, and therefore the initially mixed monolayer phase becomes demixed (i.e., A-rich). Since Γ along $T_{\rm I}$ and $T_{\rm II}$ remains finite all the way to $\mu - \mu_{x}^{\infty}(T_{\rm II}) \to 0^{-}$, we are again dealing with cases of partial wetting.

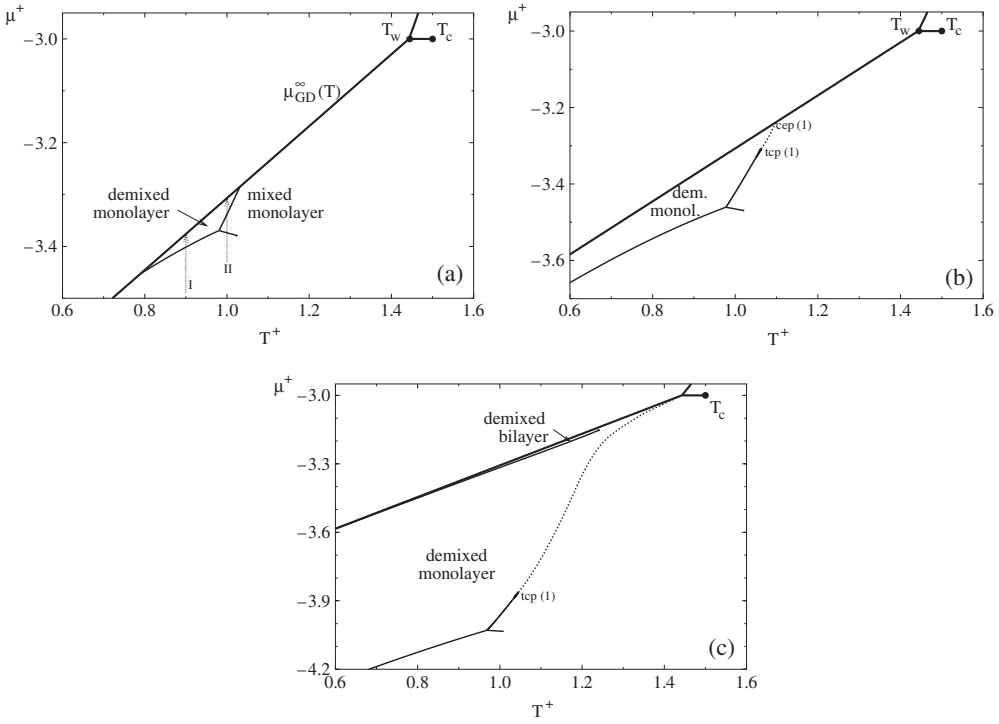

Figure 6. As figure 2 but for $|\epsilon^{*}_{AB}| = 0.5$. (a) $|\epsilon^{+}_{W}| = 1.3$; (b) $|\epsilon^{+}_{W}| = 1.4$; (c) $|\epsilon^{+}_{W}| = 2.0$.

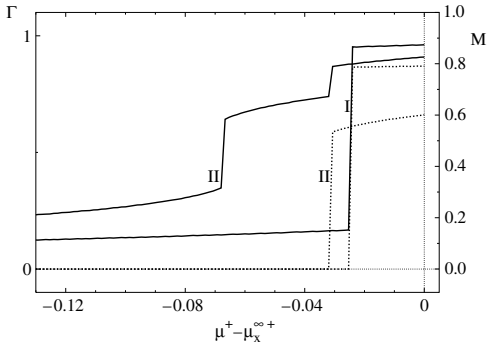

Figure 7. As figure 5 but for the two isotherms specified in figure 6(a).

As $|\epsilon^{+}_{W}|$ increases to 1.4 the one-phase region of the demixed monolayer film widens considerably, as the plot in figure 6(b) shows. Between mixed and demixed monolayer films, continuous as well as discontinuous phase transitions are possible. This is because a surface tricritical point appears at $T^{+}_{tcp} \simeq 1.06$ and $\mu^{+}_{tcp} \simeq -3.31$. Between the tricritical point and the bulk coexistence curve, a new surface λ-line arises, as the plot in figure 6(b) shows.

Further increase of $|\epsilon_{W}|$ causes the monolayer coexistence lines to become even more 'detached' from the bulk phase diagram, as the plots for $|\epsilon^{+}_{W}| = 2.0$ in figure 6(c) show. Hence, the λ-line also visible in figure 6(c) becomes longer compared with its counterpart in figure 6(b). In addition to these, somewhat less spectacular features, a novel demixed bilayer

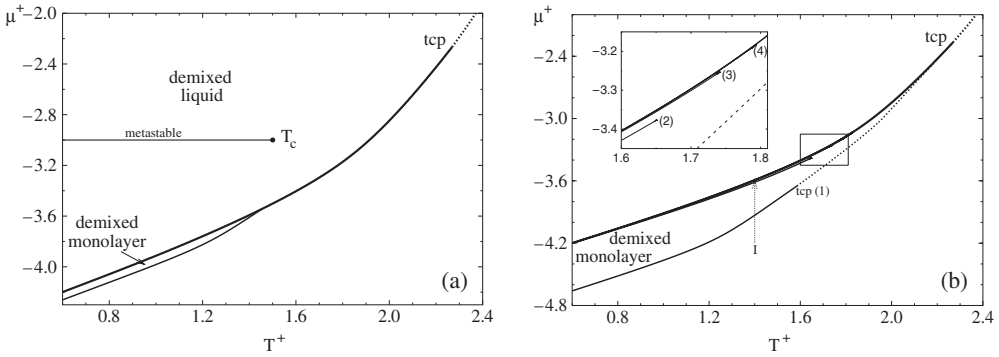

Figure 8. As figure 2, but for $|\epsilon^*_{\rm AB}| = 0.3$. (a) $|\epsilon^+_{\rm W}| = 1.6$; also shown is the (metastable) coexistence line $\mu^\infty_{\rm GM}(T)$. (b) $|\epsilon^+_{\rm W}| = 2.0$; the inset is an enhancement of the small rectangular region showing that an (infinite) number of layering transitions *below* the bulk coexistence line exist.

film arises as a thermodynamically stable phase in figure 6(c). Unlike the bilayer films for $|\epsilon^*_{\rm AB}| = 0.7$, mixed bilayers are presently not observed. The appearance of such multilayer films will become a key issue in the next section 5.2.3.

5.2.3. The case $|\epsilon^*_{\rm AB}| = 0.3$. We begin with a fluid–substrate attraction $|\epsilon^+_{\rm W}| = 1.6$ for which we plot $\mu^\infty_x(T)$ in figure 8(a). The attraction between unlike molecules of both species $|\epsilon^*_{\rm AB}| = 0.3$ is already sufficiently weak to promote a strong tendency of the bulk mixture to phase separate. This is indicated in figure 8(a), where we plot the coexistence line between the metastable gas and mixed liquid phases which turns out to be 'buried' deep inside the one-phase region of the demixed liquid phase, thus being entirely inaccessible from an equilibrium perspective. That is, with respect to $\mu^\infty_x(T)$ plotted in figure 8(a), $\mu_{\rm GM}(T)$ turns out to be metastable. Consequently, the critical end point characteristic of the previously discussed cases has disappeared. Instead a bulk tricritical point (tcp) is visible in the plot of figure 8(a), where both the demixed liquid and the gas become critical. In addition, only a demixed monolayer film is adsorbed on the solid substrate.

If we now increase the fluid–substrate attraction to $|\epsilon^+_{\rm W}| = 2.0$, the one-phase region of the demixed monolayer film widens. The coexistence line $\mu_{Gd1}(T)$ ends at a new tricritical point located at $T^+_{\rm tcp}(1) \simeq 1.58$, $\mu^+_{\rm tcp}(1) \simeq -3.65$ (see figure 8(b)). At this tricritical point a surface λ-line starts separating the gas from the demixed monolayer. However, the inset in figure 8(b) shows that a number of additional layer-coexistence lines arise, too. Consider now the isotherm labelled I in figure 8(b). The corresponding plot of Γ in figure 9 exhibits a discontinuous increase at $\mu^+ - \mu^{\infty+}_x(T_{\rm I}) \simeq -0.34$, where the isotherm crosses the coexistence line of the demixed monolayer film. That this film is, in fact, demixed is reflected by the simultaneous pronounced, discontinuous increase of M to a value of about 0.65 (see figure 9). As we move closer towards bulk gas–liquid coexistence along $T_{\rm I} = 1.4$, additional layering transitions are visible in the plot of Γ which tends to diverge at bulk gas–liquid coexistence. Because M increases discontinuously as well, the newly formed thicker films are even more demixed.

Hence, in this case we have complete wetting of the solid substrate above $T = 0$ in accord with the qualitative argument put forward in section 4.2.2, where we argued that on account of decomposition at sufficiently low temperatures complete wetting should be possible along the entire bulk coexistence line $\mu^\infty_{\rm GD}(T)$. On the basis of figures 4(b), 5(b), and 8(b), we

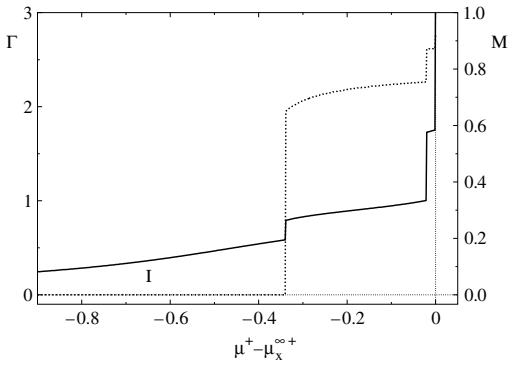

Figure 9. As figure 5 but for the isotherm specified in figure 8(b).

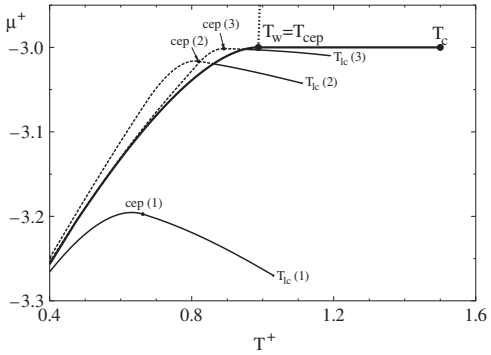

Figure 10. As figure 2, but for $|\epsilon^*_{AB}| = 0.7$ and $|\epsilon^+_W| = 1.18$. Also shown are a number of layering coexistence lines where metastable and thermodynamically stable portions are represented by dotted and full curves, respectively. Surface λ-lines starting at surface critical end points cep(n) have been omitted for the sake of clarity.

are now also in a position to unravel the ostensible contradiction between the prediction of complete wetting at temperatures *below* T_{cep} and the scaling argument sketched in section 4.3. Comparing first $\mu_x(T)$ in figures 4(b) and 8(b), we notice that increasing $|\epsilon_W|$ and lowering $|\epsilon_{AB}|$ causes a complete change in topology of the phase diagram in that only demixed film or bulk liquid phases are present in figure 8(b). Therefore, unlike $\mu_x(T)$ plotted in figure 4(b), the phase diagram shown in figure 8(b) does not exhibit a critical end point, and hence the scaling argument becomes inapplicable to this situation. As a consequence no restrictions are imposed on the location of T_w, in accord with our findings.

However, we notice from figures 4(b) and (c) that the layering temperatures may be lower than T_{cep}. A more detailed analysis of the various layering coexistence lines provides a means of understanding why T_w can never be lower than T_{cep}, in addition to the scaling argument of section 4.3. A plot of $\mu_x^\infty(T)$ in figure 10 illustrates that for $|\epsilon^*_{AB}| = 0.70$ and $|\epsilon^+_W| = 1.18$ only the gas–monolayer coexistence line is at chemical potentials *lower* than that of $\mu^\infty_{GD}(T)$. Bi- and trilayer coexistence lines have only certain parts below the bulk coexistence line, that is the monolayer film is thermodynamically stable over the entire temperature range $0 \leqslant T \leqslant T_{lc}(1)$. Thus, if one approaches the bulk coexistence line from below along an isotherm $T < T_{cep}$, this isotherm will intersect only a *finite* number of layer coexistence lines and therefore Γ cannot diverge to infinity as would be required in the case of complete wetting. Only for

$T \geqslant T_{\mathrm{cep}}$ are *all* layer coexistence lines below the bulk coexistence line $\mu_{\mathrm{GD}}(T)$. Hence, if one approaches $\mu_x^{\infty}(T)$ an isotherm will intersect an infinite number of layer coexistence lines, and consequently Γ diverges to infinity for all $T \geqslant T_{\mathrm{cep}}$. In other words, the relative stability of layering transitions with respect to $\mu_x^{\infty}(T)$ determines the temperature range over which one can expect complete wetting.

6. Discussion and conclusions

We have studied the wetting of nonselective, planar substrates by symmetric binary mixtures using mean-field lattice density functional theory. By varying the attraction strength between unlike molecules, ϵ_{AB}, and that between a molecule and the substrate, ϵ_{W}, we observe a rich wetting behaviour. Through an analytical calculation of the chemical potential at coexistence for mixed and demixed films of various thicknesses at $T = 0$ we identify two 'natural' energy scales of our model. One is posed by the attraction between like molecules ϵ_{AA} and becomes relevant if the adsorbed film demixes or if it consists of a pure fluid (i.e., for $|\epsilon_{\mathrm{AB}}^*| = 1$). The other one, $\overline{\epsilon}$, arises in mixed films and depends on both ϵ_{AA} and ϵ_{AB} (see (3.6)).

Based on simple energetic arguments we derived a condition for complete wetting in the limit of vanishing temperature (see (4.6)). In the case of a mixed film $\epsilon_{\mathrm{liq}} = \overline{\epsilon}$. For example, if the binary mixture degenerates into a pure fluid (i.e., for $|\epsilon_{\mathrm{AB}}^*| = 1$) we expect the wetting temperature to vanish if $|\epsilon^+| = 1.0$ on account of (4.6), which is confirmed by results plotted in figure 2(c).

For $|\epsilon_{\mathrm{AB}}^*| < 1$, thermodynamically stable films always decompose for sufficiently low temperatures. The transition between mixed and demixed films can be continuous or discontinuous (see figure 4). Upon decomposition the energy scale posed by $\epsilon_{\mathrm{liq}} = \epsilon_{\mathrm{AA}}$ becomes relevant. However, $|\epsilon_{\mathrm{AA}}| > |\overline{\epsilon}|$ such that the inequality stated in (4.6) may be invalidated. To observe complete wetting by demixed films for $T = 0$ in this latter case, the fluid–substrate attraction needs to be raised accordingly.

The key result of this work is that the wetting temperature T_{w} may vanish in the limits $|\epsilon_{\mathrm{AB}}^*| = 1$ (pure fluid) and $|\epsilon_{\mathrm{AB}}^*| \to 0$ (see figures 2(c) and 8(b)) if the fluid–wall attraction is adjusted properly. In other words, in both cases we observe complete wetting if the gas–liquid coexistence line is approached along any isotherm $T \geqslant 0$. Again, in the limit $T = 0$ the latter is demonstrated analytically in section 4.2.

For intermediate values of ϵ_{AB}, however, T_{w} has a lower bound $T_{\mathrm{cep}} > 0$, in accordance with scaling-law predictions [45–48]. The existence of a lower bound $T_{\mathrm{w}} \geqslant T_{\mathrm{cep}}$ can be rationalized in terms of the dependence of the topology of $\mu_x(T)$ on both ϵ_{AB} and ϵ_{W}. Focusing on the bulk phase diagram first (i.e., for $\epsilon_{\mathrm{W}} = 0$) one realizes for a pure fluid, where $|\epsilon_{\mathrm{AB}}^*| = 1$, only gas and liquid phases coexist along $\mu_x^{\infty +} = -3$ and $0 \leqslant T \leqslant T_{\mathrm{c}}$. If $|\epsilon_{\mathrm{AB}}^*| < 1$, a critical end point at a temperature T_{cep} arises, where a λ-line intersects $\mu_x^{\infty}(T)$ such that mixed and demixed liquid phases are separated by a line of continuous phase transitions. In this case $\mu_{\mathrm{GM}}^+ = -3$ only for $T \geqslant T_{\mathrm{cep}}$, whereas $\mu_{\mathrm{GD}}^+(T) \leqslant -3$ for $T \leqslant T_{\mathrm{cep}}$ such that $\mathrm{d}\mu_{\mathrm{GD}}(T)/\mathrm{d}T \geqslant 0$ over this temperature range. The coexistence line μ_{GM} ends at the critical point where $T_{\mathrm{c}}^+ = \frac{3}{2}$, and gaseous and mixed liquid phases become indistinguishable. As $|\epsilon_{\mathrm{AB}}|$ decreases, T_{cep} shifts to higher temperatures and is eventually transformed into a tricritical point $(\mu_{\mathrm{tcp}}, T_{\mathrm{tcp}})$, where coexisting mixed and demixed liquid become critical. Lowering $|\epsilon_{\mathrm{AB}}|$ even more causes T_{c} to vanish such that eventually only demixed liquid and gaseous phases coexist.

For intermediate values ϵ_{AB}, where $T_{\mathrm{cep}} < T_{\mathrm{c}}$, one may now introduce a planar substrate surface with $\epsilon_{\mathrm{W}} \lesssim 0$. The discussion in section 4.2.2 showed that for $T = 0$ films adsorbed on such a surface will demix spontaneously regardless of their thickness (see equations (4.8), (4.15)) such that at $T = 0$ we have a multiphase point in the sense that there

is no difference in stability between the demixed bulk liquid and adsorbed films of arbitrary thickness. However, for infinitesimally larger temperatures $T \gtrsim 0$, the demixed liquid bulk phase turns out to be more stable than any film adsorbed on the solid substrate. Hence, we have only partial wetting for $T \gtrsim 0$.

As T increases along the layer coexistence lines each film exhibits a critical end point $T_{\mathrm{cep}}(k)$, where a (surface) λ-line starts (see figures 4(c), (d), and 10). For $T \gtrsim T_{\mathrm{cep}}(k)$, a film of k layers turns out to be mixed because entropic contributions dominate energetic ones. This is the easier the lower k is, such that $\lim_{k\to\infty} T_{\mathrm{cep}}(k) = T_{\mathrm{cep}}$. The mixed films eventually become more stable than the demixed liquid bulk phase (see figure 10). Thus, one has layering temperatures $T_{\mathrm{l}}(k)$, but only for finite k as long as $T < T_{\mathrm{cep}}$. Consequently, there is no complete wetting below the bulk critical end point, in accord with the scaling predictions summarized in section 4.3.

The main observations of this work can thus be summarized as follows.

(i) Complete wetting of solid surfaces by *mixed* films occurs only for temperatures $T \geqslant T_{\mathrm{cep}}$ regardless of ϵ_{AB} and ϵ_{W}. Both parameters do, of course, affect the specific location of the critical end point.

(ii) If complete wetting occurs for arbitrary temperatures $0 \leqslant T \lesssim T_{\mathrm{c}}$, it requires *demixed* films as an ineluctable prerequisite. However, such decomposition requires sufficiently attractive substrates relative to the strength of the A–B attraction, that is sufficiently large $|\epsilon_{\mathrm{W}}^{+}|$ or small $|\epsilon_{\mathrm{AB}}^{*}|$. However, such a choice of parameters is more likely to cause mixed liquid bulk phases to be absent, so that a critical end point does not even exist. In this case no restrictions are imposed *in principle* on the wetting temperature.

Our results are in qualitative agreement with those obtained earlier by Schmid and Wilding [40]. For example, for a sufficiently large value of $|\epsilon_{\mathrm{W}}|$ these authors report a discontinuous change in film thickness accompanied with a change in its composition (see figure 14 of [40]). This feature has also been observed here (see figures 6(a), 7, isotherm II or figure 4(d)) where, however, the film thickness changes at most from mono- to bilayer (see figure 4(d)) on account of the short-range attraction employed in this study. A much larger increase in film thickness is observed by Schmid and Wilding in their grand canonical ensemble Monte Carlo simulations. If $|\epsilon_{\mathrm{W}}|$ becomes sufficiently large, Schmid and Wilding observe a 'weakening' of the wetting transition (see figures 13, 14 of [40]). This effect is also observed here. Consider, for example, the isotherm $T = 1.05$ in figures 6(b) and (c), which is slightly below and above the tricritical point cep(1), respectively. Hence the order of the layering transition changes from discontinuous to continuous along this isotherm as $|\epsilon_{\mathrm{W}}^{+}|$ increases from 1.4 to 2.0. However, the reader should note that the present study goes beyond that of Schmid and Wilding [40], who fixed $|\epsilon_{\mathrm{AB}}^{*}|$ near 0.7 and varied only ϵ_{W}, whereas the impact of the variation of parameters is investigated here.

Acknowledgments

We thank Professor Peter A Monson (University of Massachusetts) for a number of helpful discussions we enjoyed during his sabbatical at the Technische Universität Berlin. Financial support from the Sonderforschungsbereich 448 'Mesoskopisch strukturierte Verbundsysteme' is also gratefully acknowledged.

References

[1] Young T 1805 *Phil. Trans. R. Soc.* **95** 65
[2] Dupré A 1869 *Theorie Mechanique de la Chaleur* (Paris: Gauthier-Villars) p 369

[3] de Gennes P G 1985 *Rev. Mod. Phys.* **57** 827
[4] Sullivan D E and Telo da Gama M M 1986 *Fluid Interfacial Phenomena* ed C A Croxton (New York: Wiley)
[5] Dietrich S 1988 *Phase Transitions and Critical Phenomena* vol 12, ed C Domb and J L Lebowitz (New York: Academic) p 1
[6] Schick M 1990 *Liquids at Interfaces* (*Les Houches Session XLVIII*) ed J Charvolin, J F Joanny and J Zinn-Justin (Amsterdam: Elsevier)
[7] Evans R and Parry A O 1990 *J. Phys.: Condens. Matter* **2** SA15
[8] Bonn D and Ross D 2001 *Rep. Prog. Phys.* **64** 1085
[9] Evans R and Chan M W 1996 *Phys. World* **9** 48
[10] Dash J G 1976 *Phys. Rev.* B **15** 3136
[11] Cahn J W 1977 *J. Chem. Phys.* **66** 3667
[12] Ebner C and Saam W F 1977 *Phys. Rev. Lett.* **38** 1486
[13] Saam W F and Ebner C *Phys. Rev.* A **17** 1768
[14] Stanley H E 1971 *Introduction to Phase Transitions and Critical Phenomena* (New York: Oxford University Press) chapter 3
[15] Nightingale M P and Indekeu J O 1985 *Phys. Rev.* B **32** 3364
[16] Ebner C and Saam W F 1987 *Phys. Rev.* B **35** 1822
[17] Kroll D M, Lipowsky R and Zia R K P 1985 *Phys. Rev.* B **32** 1862
[18] Lipowsky R and Seifert U 1985 *Phys. Rev.* B **31** 4701
[19] Dietrich S and Schick M 1986 *Phys. Rev.* B **33** 4952
[20] Dietrich S and Napiórkowski M 1991 *Phys. Rev.* E **43** 1861
[21] Evans R 1990 *Liquids at Interfaces* (*Les Houches Session XLVIII*) ed J Charvolin, J F Joanny and J Zinn-Justin (Amsterdam: North-Holland) p 1
[22] Pandit R, Schick M and Wortis M 1982 *Phys. Rev.* B **26** 5112
[23] Binder K and Landau D P 1988 *Phys. Rev.* B **37** 1745
[24] Schöll-Paschinger E, Levesque D, Weis J-J and Kahl G 2001 *Phys. Rev.* E **64** 011502
[25] Sliwinska-Bartkowiak M, Sowers S L and Gubbins K E 1996 *Langmuir* **13** 1182
[26] Martinez A, Pizio O, Patrykiejew A and Sokolowski S 2003 *J. Phys.: Condens. Matter* **15** 2269
[27] Woywod D and Schoen M 2003 *Phys. Rev.* E **67** 026122
[28] Patrykiejew A, Salamacha L, Sokolowski S and Pizio O 2003 *Phys. Rev.* E **67** 061603
[29] Kierlik E, Rosinberg M L, Fan Y and Monson P A 1994 *J. Chem. Phys.* **101** 10947
[30] Kellay H, Bonn D and Meunier J 1993 *Phys. Rev. Lett.* **71** 2607
[31] Beysens D and Estevé D 1985 *Phys. Rev. Lett.* **54** 2123
[32] Plech A, Klemradt U, Huber M and Peisl J 1999 *Europhys. Lett.* **49** 583
[33] Plech A, Klemradt U and Peisl J 2001 *J. Phys.: Condens. Matter* **13** 5563
[34] Plech A, Klemradt U, Aspelmeyer M, Huber M and Peisl J 2002 *Phys. Rev.* E **65** 061604
[35] Sallami H, Hamraoui A, Privat M and Olier R 1998 *Langmuir* **14** 2402
[36] Telo da Gama M M and Evans R 1982 *Mol. Phys.* **48** 687
[37] Fan Y, Finn J E and Monson P A 1993 *J. Chem. Phys.* **99** 8238
[38] Ball P C and Evans R 1988 *J. Chem. Phys.* **89** 4412
[39] Hadjiagapiou I and Evans R 1985 *Mol. Phys.* **54** 383
[40] Schmid F and Wilding N B 2001 *Phys. Rev.* E **63** 031201
[41] Silbermann J R, Woywod D and Schoen M 2004 *Phys. Rev.* E **69** 031606
[42] Lavis D A and Bell G M 1989 *Statistical Mechanics of Lattice Models* vol 1 *Closed-Form and Exact Solutions* (Berlin: Springer) p 60
[43] Baxter R J 1990 *Exactly Solved Models in Statistical Mechanics* (London: Academic) chapter 3
[44] Rowlinson J S and Widom B 1984 *Molecular Theory of Capillarity* (Oxford: Oxford University Press)
[45] Fisher M E and Upton P J 1990 *Phys. Rev. Lett.* **65** 2402
[46] Fisher M E and Barbosa M C 1991 *Phys. Rev.* B **43** 11177
[47] Wilding N B 1997 *Phys. Rev. Lett.* **78** 1488
[48] Wilding N B 1997 *Phys. Rev.* E **55** 6624